EXTENDED EXPERIMENTAL PROCEDURES

Cell Culture

HEK293T (called 293T throughout) and hTERT-RPE-1 (called RPE throughout) cells were maintained in DMEM with 10% fetal bovine serum, 1% penicillin/streptomycin, and L-glutamine. Stable 293T cell lines were generated as in (Black et al., 2010). Stable RPE cell lines were generated by retroviral transduction of MSCV-GFP or MSCV-GFP-KDM4A. Cells were selected for 96 hours with puromycin. All experiments on stable cells were performed after two months of culture post infection with KDM4A. Transient transfection experiments were performed using Roche X-tremeGENE 9 DNA transfection reagent in OPTI-MEM I media (Gibco) for four hours. Media was then replaced with standard DMEM. For concomitant overexpression and depletion in 293T cells, shRNA was transfected for 4 hours, cells recovered in DMEM for 20 hours and cells were transfected a second time with additional shRNA and KDM4A expression plasmid. Cells were harvested for FISH 48 hours following the second transfection. No selection was used in transient transfection experiments.

Expression Plasmids

The pFN21A clone expressing an N-Terminal HaloTag fusion of human full-length KDM4A or Suv39h1 (NM_014663) was obtained from Kazusa DNA Research Institute (Kisarazu, Japan). HaloTag (ADN27525.1) control vector (Promega) was used for expression of the HaloTag protein alone. MSCV-GFP-KDM4A, MSCV-GFP-H188A, MSCV-RFP-HP1, pSuper and pSuper sh2A.1 constructs were made as described (Black et al., 2010). N-terminal HA-FLAG (NHF) deletion constructs were generated using primers at the indicated amino acid residues and cloned into pEntry using Gateway technology (Invitrogen). Fragments were transferred to N-terminal HA-FLAG (NHF) destination vector following the manufacturer's instructions. H188A contains two point mutations to eliminate catalytic activity H188A and W208R (Black et al., 2010). All clones were sequence verified.

Western Blots

Western blots were performed as in (Black et al., 2010). Antibodies used were: KDM4A (Neuro mAB, 75-189), β-actin (Millipore), GFP (Neuro mAB, 73-131), RFP (Abcam, ab62341), p53 (Santa Cruz, sc-126), MCM2 (Cell Signaling, #3619S), MCM3 (Cell Signaling, #4012S), MCM7 (Cell Signaling, #3735S), Halo (Promega), Actinin (Santa Cruz, sc-17829), HA 12CA5 (Roche), FLAG M2 (Sigma), DNA Pol α (Abcam, ab31777).

G-Band and Spectral Karyotyping

G-Band analysis was performed and analyzed by WiCell Cytogenetics Institute (Wisconsin). SKY and corresponding analysis was performed by Cristina Montagna in the Molecular Cytogenetic Core at Albert Einstein College of Medicine. The RPE stable cell lines were analyzed by SKY two independent times: once after six months in culture and a second time after an additional three months of culture.

Subcellular localization and Catalytic Activity of KDM4A deletion fragments

The indicated NHF-tagged KDM4A deletion constructs were transfected into RPE cells grown on coverslips in 10 cm dishes using X-tremeGENE 9 DNA transfection reagent (Roche). H3K36me3 and subcellular localization were assayed by examining transfected cells (positive for HA staining; HA.11 Covance) following fixation in 3.7% PFA in PBS (Whetstine et al., 2006).

Immunoprecipitation and Chromatin Immunoprecipitation

Immunoprecipitations were performed essentially as described in (Van Rechem et al., 2011). Briefly, cells were lysed in cellular lysis buffer (5mM PIPES, 85mM KCl, 0.5% NP40) and nuclei

were collected following centrifugation. Nuclei were lysed in IPH buffer with sonication, lysates were cleared and immunoprecipitations were performed in the presence of 100ug/ml ethidium bromide and digested with 0.25ul benzonase to eliminate protein-nucleic acid interactions. Immunoprecipitation from 293T cells were carried out in IPH with 150mM NaCl and from RPE cells in 300mM NaCl. Immunoprecipitation of HaloTag polymerase subunits with endogenous KDM4A was performed according to the manufacturers protocol (Promega) with minor modification. Whole cell lysates were prepared using sonication of cells in Halo lysis buffer. Immunoprecipitations were performed with ethidium bromide overnight at 4˚C. Elution was performed using SDS sample loading buffer.

Chromatin immunoprecipitations were performed as in (Black et al., 2010) with some minor changes. Sonication was performed using a Qsonica Q800R system with a constant chiller. For ChIP, RPE cells were arrested in 2mM HU for 20 hours prior to crosslinking to assess enrichment in KDM4A, HP1γ, H3K9me3, H3K36me3, and DNA polymerase α at G1/S transition. For release from HU (as indicated in figures), HU containing media was removed by aspiration, and cells were rinsed twice with fresh DMEM prior to addition of fresh DMEM for release for the indicated times. 1 to 10ug of chromatin was used for each IP, which was dependent on the antibody used. For HP1γ, chromatin was prepared and sonicated in TE with 1%SDS, diluted to 0.2% SDS prior to dilution for the immunoprecipitation. Chromatin for histone ChIP was prepared and sonicated in TE with 1% SDS. Chromatin for KDM4A, Polα, and MCM7 was prepared and sonicated in TE with 0.2% SDS. Prior to ChIP, RPE chromatin was precleared for one hour with protein A agarose, and for one hour with magnetic protein A or G beads (Invitrogen; to match antibody type). Immunoprecipitated DNA was purified using either PCR Purification Columns (Promega) or AMPureXP. Data presented are averages from the two independently prepared polyclonal RPE cell lines from at least two independent chromatin preparations per cell line. Antibodies used for ChIP are as follows: DNA Polα (Abcam, ab31777 lot 290601), MCM7 (Cell Signaling, #3735S lots 02/2013 and 03/2013), KDM4A (Black et al., 2010), HP1γ (Millipore, 05-690 lot DAM1501782), H3K9me3 (Abcam, ab8898 lot GR30928-1), H3K36me3 (Abcam, ab9050 lot GR10860-1), H3 (Abcam, ab1791 lot GR63387-1).

Fluorescent In Situ Hybridization (FISH)

FISH was performed as described in (Manning et al., 2010). Probes for 1q12h, 1q telomere, 6p21/chr14 IGH translocation and chromosome 2, 6, 8, and X alpha satellite were purchased from Rainbow Scientific. Probes for 1q12 (RP11-17L12), Xq13.2 (RP11-451A22), Xq13.1 (RP11-177A4) were purchased as BAC clones from Children's Hospital Oakland Research Institute (CHORI BacPac) FISH verified clone repository. Oligonucleotide probes for 1q21.2 (BCL9) and 1q23.3 were purchased from Agilent (SureFISH). BACS were prepared utilizing PureLink HiPure Plasmid Filter Maxiprep kit (Life Technologies) using the recommended modified wash buffer. Probes were nick translated (Abbot Molecular Kit) in the presence of fluorescently labeled dTTP (Enzo Life Science). Images of multiple planes of fields of nuclei were acquired on an Olympus IX81 Spinning Disk Microscope and analyzed using Slidebook 5.0 software. We used a conservative scoring metric for copy gain. Any foci that were touching were scored as a single foci to prevent increased numbers due to normally replicated foci. For RPE cells, copy gain was scored as any cell with 3 or more distinct foci. For 293T cells, copy gain was scored for any cell with 5 or more distinct foci. For RPE cells each experiment includes at least one replicate from the two different polyclonal stable cell preparations. At least 100 cells for each replicate were scored for all experiments except analysis of single cell clones.

Infection with Histone H3.3 variants.

Lentiviral stocks provided from the Allis lab were used to infect RPE cells in the presence of 8μg/ml polybrene for 8 hours (Lewis et al., 2013). Cells were washed 2 times with DMEM.

Cells were collected 24 hours later for analysis by FISH and western blot. Incorporation of histone variants was confirmed by subcellular fractionation and western blotting.

Fluorescent In Situ Hybridization (FISH) coupled to Chromosome 1 Paint

FISH/Paint was performed using the 1q12/21 probe labeled in Spectrum Orange combined with a chromosome 1 painting probe labeled in Spectrum Green. The chromosome paint probe was generated using standard protocols (Montagna et al., 2002). Equal volumes of locus specific and paint probe resuspended in hybridization solution (50% dextran sulfate/2× SSC) were combined and denatured at 85°C for 5 min, applied to the slides and incubated overnight at 37°C in a humidified chamber. Before hybridization the slides with interphase nuclei were denatured with 50% formamide/2× SSC at 80°C for 1.5 min and then dehydrated with serial ethanol washing steps (ice cold 70%, 90% and 100% for 3 min each). After hybridization the slides were washed three times for 5 min with 50% formamide/2× SSC, 1× SSC and 4× SSC/0.1%Tween. Slides were dehydrated with serial ethanol washing steps (as above) and mounted with ProLong Gold antifade reagent with DAPI (Invitrogen) for imaging. FISH/Paint images were acquired with a manual inverted fluorescence microscope (Axiovert 200, Zeiss) with fine focusing oil immersion lens (×40, NA 1.3 oil and ×60, NA 1.35 oil). Multiple focal planes were acquired for each channel to ensure that signals on different focal planes were included. The resulting fluorescence emissions were collected using 425–475 nm (for DAPI), 546–600 nm (for spectrum orange), and 500–550 nm (for AlexaFluor488) filters. The microscope was equipped with a Camera Hall 100 and the Applied Spectral Imaging software.

Cesium Chloride Gradient Centrifugation

RPE cells were treated with 100μM BrdU 14 hours prior to harvest. Cells were lysed in RIPA supplemented with 100μg of RNAse A (Fisher) for 2 hours at 37 degrees Celsius. Buffer was supplemented to 1% SDS and 20 μg of proteinase K was added and digested overnight at 55 degrees Celsius. DNA was extracted three times with phenol:chloroform:isoamyl alcohol and ethanol precipitated. Precipitated DNA (approximately 300 μg) was resuspended in NEB buffer 2 supplemented with RNAse A and digested with 200U of EcoRI and BamHI (NEB) overnight at 37 degrees Celsius. Digests were supplemented to 1% SDS and digested with 10 μg of proteinase K for 1 hour at 55 degrees Celsius. DNA was extracted with phenol:chloroform:isoamyl alcohol and ethanol precipitated. Precipitated DNA was resuspended in TE and concentration determined by Nanodrop. 100 μg of DNA was mixed with 1g/ml CsCl in TE (refractive index of 1.4015-1.4031) in Quick-Seal ultracentrifuge tubes (Beckman). The CsCl gradient was centrifuged at 44,400 RPM in a VTi-65 rotor for 72 hours at 25 degrees Celsius. Fractions were collected from the bottom of the gradient in ~200 μl aliquots. DNA concentration of each fraction was measured by Nanodrop. Appropriate fractions were pooled, dialyzed against 0.1X TE and concentrated by dialysis against 0.1XTE with 40% glycerol. Concentrated pools were ethanol precipitated and resuspended in ddH2O prior to analysis by quantitative PCR (qPCR). Each re-replicated fraction was diluted to 15ng/ul stock and 7.5ng of re-replicated DNA pool was analyzed by qPCR on a Roche LC480 using FastStart Universal SYBR Green Master Mix (Roche) following the manufacturer's instructions. 7.5ng of input DNA was analyzed by qPCR at the same time. Each sample was normalized to its own input prior to determination of fold-change in re-replication. Primers used in this study will be provided upon request.

HaloTag Mammalian Pull-Down Assay for Mass Spectrometry

HEK293T cells (12 x 10^6 cells) were plated in a 150 mm dish and grown to 70-80% confluence (approximately 18 hours). The cells were then transfected with 30μg of plasmid DNA using FuGENE HD Transfection Reagent (Promega) for 24 hours, according to manufacturer's protocol. Cells expressing Halo-KDM4A or Halo-CTRL were incubated in mammalian lysis

buffer (50mM Tris-HCl, pH 7.5, 150mM NaCl, 1% Triton X-100, and 0.1% sodium deoxycholate) supplemented with Protease Inhibitor cocktail (Promega) and RQ1 RNAse-Free DNAse (Promega) for 10 minutes on ice. Lysate was then homogenized with a syringe and centrifuged at 14.000 x g for 5 minutes to pellet cellular debris. Clarified lysate was incubated with HaloLink Resin (Promega) that had been pre-equilibrated in resin wash buffer (TBS and 0.05% IGEPAL CA-640 (Sigma)) for 15 minutes at 22^{o}C with rotation. Resin was then washed 5 times with wash buffer, and protein interactors were eluted with SDS elution buffer (50mM Tris-HCl, pH 7.5, and 1% SDS).

Mass Spectrometry Analysis

HaloTag pulldown purified complexes were analyzed and processed by MS Bioworks, LLC (Ann Arbor, Michigan). The samples were separated on a SDS-PAGE gel, which was then Coomassie stained and cut into 10 fragments. Each gel piece was processed with the Progest Protein Digestion Station (Digilab). Briefly, gel slices were washed using 25 mM ammonium bicarbonate and acetonitrile, followed by reduction with 10 mM dithiothreitol, and alkylation with 50 mM iodoacetamide. Proteins were digested with trypsin (Promega) for 4 hours and digestion was quenched with formic acid. Gel digests were analyzed directly by nano LC/MS/MS with a NanoAcquity HPLC (Waters) interfaced with an Orbitrap Velos Pro (Thermo Scientific) tandem mass spectrometer. Digested peptides were loaded on a trapping column and eluted over a 75 µm analytical column packed with Jupiter Proteo Resin (Phenomenex) at 350nl/min. The mass spectrometer was operated in data-dependent mode, with MS performed in the Orbitrap at 60.000 full width at half maximum (FWHM) resolution, and MS/MS performed in the LTQ. The 15 most abundant ions were selected for MS/MS. The data were searched with Mascot (Matrix Science) against the concatenated forward/decoy UniProt Human Database, and Mascot DAT files were visualized and filtered by Scaffold (Proteome Software). Data were filtered using a minimum protein value of 90%, a minimum peptide value of 50% (Protein and Peptide Prophet scores), and required at least two unique peptides per protein. Spectral counting was performed and normalized spectral abundance factors determined. Data were reported at less than 1% false discovery rate (FDR) at the protein level based on counting the number of forward and decoy matches. Interacting proteins were analyzed using IPA for pathway analysis (Ingenuity Systems).

Flow Cytometry Analysis of Cell Cycle and Apoptosis

Asynchronously growing, or G1/S or G2 arrested cells were prepared and fixed as in (Black et al., 2010). Cell cycle was analyzed by PI staining and analyzed using a BD FACS ARIA II. Apoptosis was determined using Annexin V and PI staining following the manufacturer's instructions (Life Technologies).

KDM4A Copy Number Determination in TCGA Data Set

The somatic copy number alterations (SCNAs) for 24,176 genes of the pan-cancer data set including 4,420 samples across multiple tumor types are annotated by GISTIC2.0 (Beroukhim et al., 2007; Beroukhim et al., 2010; Network, 2008). The copy number change in each gene is defined as possessing deep deletion (-2), shallow deletions (-1), neutral copy number (0), low gain (+1), and high gain (+2) in each sample using sample-specific thresholds. High gains are segments with copy number that exceed the maximum median chromosomal arm copy number for that sample by at least 0.1; low gains are segments with copy numbers from 2.1 to the high gain threshold; neutral segments have copy numbers between 1.9 and 2.1; shallow losses have copy numbers between 1.9 and the deep deletion threshold; and deep deletion have copy numbers that are below the minimum median chromosomal arm copy number for that sample by at least 0.1.

KDM4A mRNA expression from RNA-seq in TCGA Data Set

Reads per kilobase of exon model per million mapped reads (RPKM) were annotated for 16,407 genes in 1953 samples across multiple tumor types. 1770 samples having both copy number and RPKM data were used to quantify an association between copy number alterations and the mRNA expression levels in KDM4A in Figure 1B and 1D, and Figure S1. The "Gain" group corresponds to the sample set with KDM4A GISTIC annotation = +1 or +2, the "No change" group corresponds to the samples set with KDM4A GISTIC annotation = 0, and the "Loss" group is associated to the sample set with KDM4A GISTIC annotation = -1 or -2.

Clinical Data in TCGA Data Set

Overall survival in 541 Ovarian Cancer samples (256 alive and 285 deceased) was defined as the interval from the date of initial surgical resection to the date of last known contact or death. The association of the KDM4A copy number status, Del (-2), Loss (-1), None (0), Gain (+1), Amp (+2) to the clinical outcome in Figure 1E through 1H was tested for 285 deceased patients by Student's t-test (one-tailed) and statistical significance was considered when $P < 0.05$.

Determination of Cytoband Copy Number and Correlation with KDM4A in TCGA Data Set

In addition to the copy number annotation for each gene, the mean focal copy number for 807 cytobands including X-chromosome were annotated in each sample by taking an average of focal copy numbers of every genes within the same cytoband. Arm-level SCNA contributions to the mean focal copy number in each cytoband were removed by only considering GISTIC annotated focal copy numbers much smaller than a chromosome arm or entire chromosome. Detecting chromosomal regions significantly co-amplified with KDM4A copy gains or amplifications was first performed by the one-tailed Student's t-test for the mean focal copy number changes between KDM4A copy-gained samples (GISTIC annotation = +1 or +2) and KDM4A copy-neutral samples (GISTIC annotation = 0) across 807 cytobands. We also calculated the significance using the gene-specific copy-number for KDM4A and KDM4B as positive controls (Figure 6A-C). We also performed the second independent test (Figure S6I-K) by approximating a null distribution of mean cytoband copy differences by a normal function $N(\mu_{12}-\mu_0, \sigma_0^2/n_0+\sigma_{12}^2/n_{12})$ where μ_0 and μ_{12} are samples means across all cytobands, σ_0^2 and σ_{12}^2 are mean sample-specific variances within each group, and n_0 and n_{12} are the number of samples in KDM4A copy-neutral and KDM4A copy-gained groups, respectively. This test is based on comparing the means of the two sets while permuting values within each of the samples (and using a Gaussian approximation). The p-values across 807 cytobands were annotated by computing the probability of more extreme differences than the corresponding cytoband copy difference in the null distribution. The empirical cumulative distribution functions (the fraction of samples below the given mean focal copy) were determined by enumerating samples having the mean focal copy number less than or equal to the value on the x-axis in Figure S6C-H for KDM4A and KDM4B amplified (+2), copy-gained (+1), and copy-neutral samples (0).

Supplemental Figure Legends

Supplemental Figure 1 (Related to Figure 1). Amplification and Overexpression of KDM4A in Cancer. (A) Analysis of RNAseq data from all cancer types indicating expression level of KDM4A relative to KDM4A copy number binned by GISTIC annotation. (B) Analysis of RNAseq data from all cancer types indicating expression level of KDM4B relative to KDM4B copy number binned by GISTIC annotation. (C) Analysis of RNAseq data from all cancer types indicating expression level of KDM4C relative to KDM4C copy number binned by GISTIC annotation. (D) Analysis of RNAseq data from all cancer types indicating expression level of KDM4D relative to KDM4D copy number binned by GISTIC annotation. (E) Analysis of RNAseq data from Breast Cancer indicating expression level of KDM4A relative to KDM4A copy number binned by GISTIC annotation. (F) Analysis of RNAseq data from Head and Neck squamous cell carcinoma indicating expression level of KDM4A relative to KDM4A copy number binned by GISTIC annotation. (G) Analysis of RNAseq data from lung adenocarcinoma indicating expression level of KDM4A relative to KDM4A copy number binned by GISTIC annotation. (H) Analysis of RNAseq data from lung squamous cell carcinoma indicating expression level of KDM4A relative to KDM4A copy number binned by GISTIC annotation. (I) Analysis of RNAseq data from ovarian cancer indicating expression level of KDM4A relative to KDM4A copy number binned by GISTIC annotation. (J) Analysis of RNAseq data from renal adenocarcinoma indicating expression level of KDM4A relative to KDM4A copy number binned by GISTIC annotation. (K) Analysis of RNAseq data from stomach adenocarcinoma indicating expression level of KDM4A relative to KDM4A copy number binned by GISTIC annotation. (L) Analysis of RNAseq data from uterine and endometrial cancer indicating expression level of KDM4A relative to KDM4A copy number binned by GISTIC annotation.

Supplemental Figure 2 (Related to Figure 2). **Enrichment of KDM4A in a specific cytogenetic band that has altered copy number.** (A) Western blot depicting expression of GFP-KDM4A in a stable 293T cell line. (B) Western blot depicting expression of GFP-KDM4A in two different polyclonal stable RPE cells. (C) Table depicting increased binding of KDM4A in chr1 q12 cytogenetic band in 293T cells overexpressing KDM4A. Enrichment in ChIP-chip data is depicted as the Z-score for the average KDM4A/Input level for each probe in the cytogenetic band. (D) FISH analysis of 293T cells stably overexpressing GFP-CTRL or GFP-KDM4A. Data are presented as percent of cells with foci number different from the mean (not 3 or 4 foci in 293T cells). (E) FISH analysis of RPE cells stably overexpressing GFP-CTRL or GFP-KDM4A. Data are presented as percent of cells with foci number different from the mean (not 2 foci in RPE cells). (F) Western blot demonstrating siRNA depletion of CapD2 and CapD3 in CTRL and KDM4A cells. GFP-CTRL and GFP-KDM4A panels for CapD2 are the same exposure from a different, non-adjacent section of the same western blot. (G) FISH analysis for 1q12h in RPE cells stably overexpressing GFP-CTRL or GFP-KDM4A treated with siRNA against condensin 1 (CAPD2) and condensing 2 (CAPD3). (H) Western analysis of p53 induction following DNA damage by Doxorubicin (1uM for 16 hrs) in GFP-CTRL (C1 and C2) or GFP-KDM4A cells (A1 and A2). (I) Induction of p53 target genes analyzed by quantitative PCR after reverse transcription from doxorubicin damaged GFP-CTRL or GFP-KDM4A cells. Data are presented as fold induction relative to its own uninduced stable cell and normalized to expression of β-actin. Error bars represent the S.E.M. * indicates $P<0.05$ using two-tailed students T-test.

Supplemental Figure 3 (Related to Figure 3). **Verification of KDM4A expression and H3.3 incorporation.** (A) Expression of KDM4A following depletion and overexpression of GFP-CTRL or GFP-KDM4A in 293T cells. (B) Expression of NHF-tagged KDM4A deletion constructs in RPE cells. Since the NC constructs lacks the KDM4A antibody epitope we show the HA

western blot for this fragment. (C) Expression of GFP-KDM4A, GFP-KDM4B, GFP-KDM4C, and GFP-KDM4D in transiently transfected RPE cells. * indicates a non-specific band. (D) Expression and incorporation into chromatin of FLAG-tagged H3.3 variants. (E) Expression of HA-FLAG-tagged H3.3 K-to-M variants reduced the corresponding tri-methylation. (F) Expression of KDM4A and Halo-Suv39h1 in transiently transfected RPE cells. (G) Expression of KDM4A and RFP-HP1γ in transiently transfected RPE cells. Panels were assembled from the same exposure from non-adjacent lanes on different sections of the same blot.

Supplemental Figure 4 (Related to Figure 4). Verification of KDM4A expression, cell cycle profile and apoptosis. (A) Expression of KDM4A and GFP-KDM4A in RPE stable clones. (B) FACS analysis demonstrating HU and G2 arrest of CTRL and KDM4A RPE stable cells. Total DNA content as measured using propidium iodide is depicted on the x-axis. (C) KDM4A overexpressing RPE cells are not more apoptotic following treatment with hydroxyurea (HU) as measured by percent Annexin V positive cells. However, 12 hours of doxorubicin treatment induces apoptosis. * indicates $P<0.05$ using two-tailed students T-test.

Supplemental Figure 5 (related to Figure 5). KDM4A associates with replication machinery and promotes re-replication of KDM4A target regions. (A) Western blots of co-immunoprecipitation of endogenous KDM4A with the indicated licensing and replication machinery in 293T Cells. (B) A representative CsCl density gradient curve used for determining re-replication of KDM4A target regions. Data are presented as the DNA concentration of the indicated fraction (X-axis) taken from the bottom of the CsCl gradient. The positions of the light:light (L:L) and heavy:light (H:L) peaks and the heavy:heavy (H:H) region taken for analysis are indicated. (C) A graph depicting the KDM4A-dependent Chr1 sat2 re-replication plotted as a percent of input DNA loaded onto the CsCl gradient.

Supplemental Figure 6 (related to Figure 6 and Figure 7). Identification of cytogenetic bands co-amplified with KDM4A in cancer. (A) Focal amplification of specific cytogenetic bands determined by the statistical test based on the null distribution of mean cytoband copy differences correlated with amplification of KDM4A in 4,420 samples across all cancers from the TCGA data set. Graph depicts the –log(10) P-value for correlation of the copy number of each cytogenetic band with the copy number of KDM4A. The blue line represents the locus of KDM4A (gene-specific significance of $P=2x10^{-142}$). (B) Focal amplification of specific cytogenetic bands determined by the statistical test based on the null distribution of mean cytoband copy differences correlated with amplification of KDM4B in 4,420 samples across all cancers from the TCGA data set. The blue dot represents the gene-specific significance of KDM4B. (C) Focal amplification of specific cytogenetic bands determined by the statistical test based on the null distribution of mean cytoband copy differences correlated with amplification of KDM4A in 547 ovarian cancer samples. The blue line represents the locus of KDM4A (gene-specific significance of $P=1.4x10^{-42}$). For each co-amplification plot, blue shaded regions indicate 1p11.2 through 1q21.3 and red dashed lines indicate Xp11.2 through Xq13.2. (D-F) Empirical cumulative distribution function (% of samples possessing mean focal copy number less than or equal to the value on the x-axis) in 1q21.1-1q21.3 with unaltered (0) copy number of KDM4A, copy Gain of KDM4A (+1), or focally Amplified KDM4A (+2). The blue dashed lines at 0.3 is a cutoff to define the fraction of co-amplified samples with KDM4A amplification in Figure 6D-I. (G-I) Same as in (D-F) but for KDM4B. (J) KDM4A overexpression increased copy number of 1q12h, 1q12/21.1 and 1q21.2 and Xq13.1 but not X cen or Xq13.2 in 293T cells. Copy number was assessed using the indicated FISH probes. (K) KDM4A-dependent re-replicated regions are bound by KDM4A. KDM4A ChIP was conducted in 293T cells at regions of re-replication. Error bars represent the S.E.M. * indicates $P<0.05$ using two-tailed students T-test.

Supplemental Figure 7 (related to Figure 7). Extra copies of 1q12/21 can be found outside of the chromosome 1 domain in interphase cells. (A-L) Combined Chromosome 1 Paint (Green) and 1q12/21 FISH (Red) demonstrates that extra copies of 1q12/21 can be found adjacent to or outside chromosome 1 domains. Scale bar represents 5μm. (M) Schematic depicting the model by which KDM4A could promote copy number gain. Our results support a model where increased expression of KDM4A promotes recruitment of KDM4A to specific genomic regions and promotes re-replication. Increased KDM4A at these loci promotes a more open chromatin environment through removal of H3K9me3 and eviction of HP1γ. Increasing levels of Suv39h1 or HP1γ is sufficient to block this altered chromatin state. These altered chromatin domains could then support re-replication through increased recruitment of MCMs and DNA polymerases, which could be facilitated directly through interactions with KDM4A. Alternatively, the more open chromatin generated by KDM4A could indirectly promote inappropriate recruitment of MCMs and DNA polymerases to unused or reused origins, thus promoting re-replication. The inappropriate re-replication within these regions could then result in head-to-tail collision of one replication fork chasing another. These collisions would then generate extrachromosomal DNA fragments. The "?" represent possibilities that need further testing.

REFERENCES

Beroukhim, R., Getz, G., Nghiemphu, L., Barretina, J., Hsueh, T., Linhart, D., Vivanco, I., Lee, J.C., Huang, J.H., Alexander, S.*, et al.* (2007). Assessing the significance of chromosomal aberrations in cancer: methodology and application to glioma. Proc Natl Acad Sci U S A *104*, 20007-20012.

Beroukhim, R., Mermel, C.H., Porter, D., Wei, G., Raychaudhuri, S., Donovan, J., Barretina, J., Boehm, J.S., Dobson, J., Urashima, M.*, et al.* (2010). The landscape of somatic copy-number alteration across human cancers. Nature *463*, 899-905.

Black, J.C., Allen, A., Van Rechem, C., Forbes, E., Longworth, M., Tschop, K., Rinehart, C., Quiton, J., Walsh, R., Smallwood, A.*, et al.* (2010). Conserved antagonism between JMJD2A/KDM4A and HP1gamma during cell cycle progression. Mol Cell *40*, 736-748.

Lewis, P.W., Muller, M.M., Koletsky, M.S., Cordero, F., Lin, S., Banaszynski, L.A., Garcia, B.A., Muir, T.W., Becher, O.J., and Allis, C.D. (2013). Inhibition of PRC2 Activity by a Gain-of-Function H3 Mutation Found in Pediatric Glioblastoma. Science.

Manning, A.L., Longworth, M.S., and Dyson, N.J. (2010). Loss of pRB causes centromere dysfunction and chromosomal instability. Genes Dev *24*, 1364-1376.

Montagna, C., Andrechek, E.R., Padilla-Nash, H., Muller, W.J., and Ried, T. (2002). Centrosome abnormalities, recurring deletions of chromosome 4, and genomic amplification of HER2/neu define mouse mammary gland adenocarcinomas induced by mutant HER2/neu. Oncogene *21*, 890-898.

Network, C.G.A.R. (2008). Comprehensive genomic characterization defines human glioblastoma genes and core pathways. Nature *455*, 1061-1068.

Van Rechem, C., Black, J.C., Abbas, T., Allen, A., Rinehart, C.A., Yuan, G.C., Dutta, A., and Whetstine, J.R. (2011). The SKP1-Cul1-F-box and leucine-rich repeat protein 4 (SCF-FbxL4) ubiquitin ligase regulates lysine demethylase 4A (KDM4A)/Jumonji domain-containing 2A (JMJD2A) protein. J Biol Chem *286*, 30462-30470.

Whetstine, J.R., Nottke, A., Lan, F., Huarte, M., Smolikov, S., Chen, Z., Spooner, E., Li, E., Zhang, G., Colaiacovo, M., and Shi, Y. (2006). Reversal of histone lysine trimethylation by the JMJD2 family of histone demethylases. Cell *125*, 467-481.

Supplemental Figure

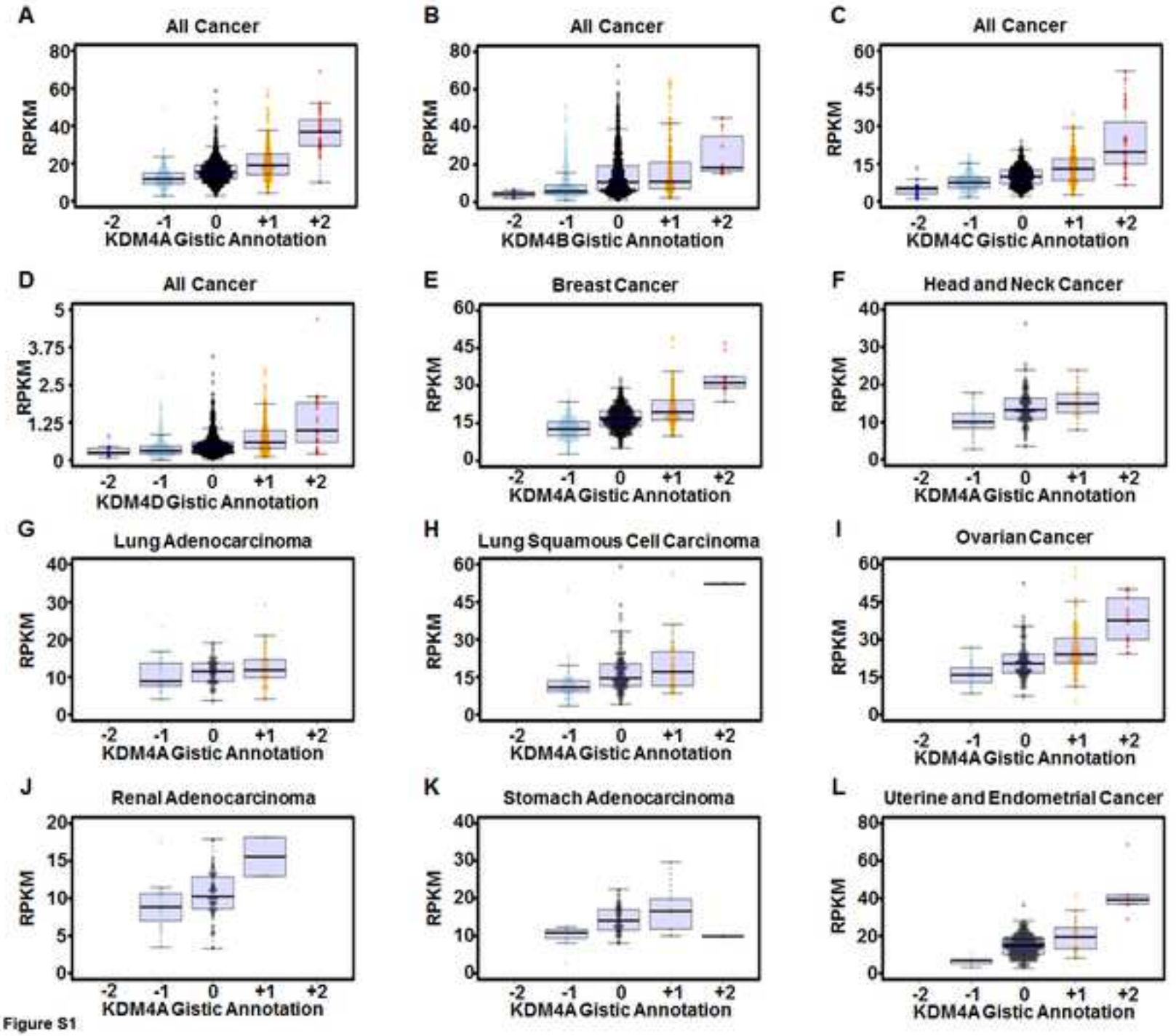

Figure S1

Supplemental Figure

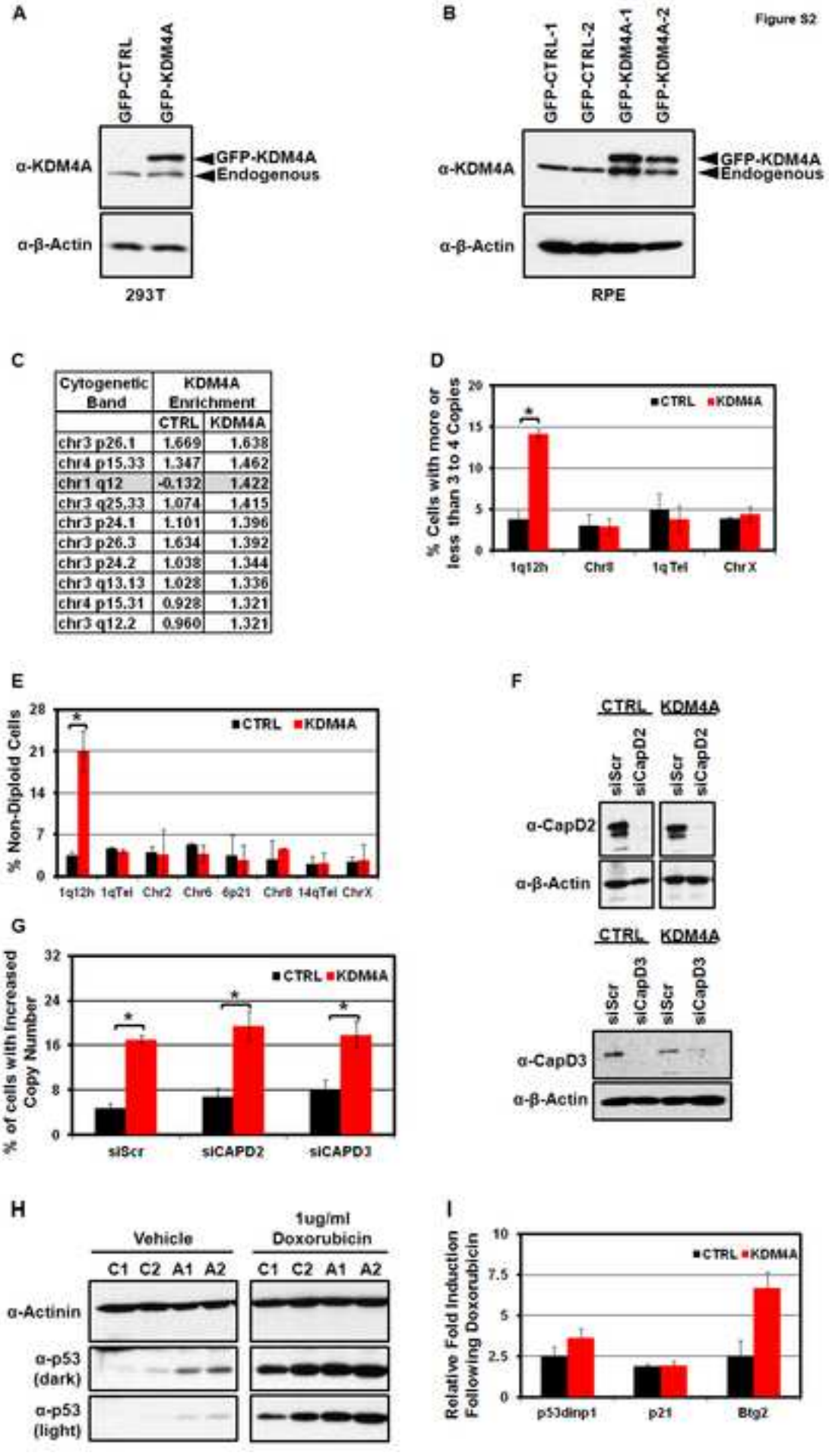

Cytogenetic Band	KDM4A Enrichment	
	CTRL	KDM4A
chr3 p26.1	1.669	1.638
chr4 p15.33	1.347	1.462
chr1 q12	-0.132	1.422
chr3 q25.33	1.074	1.415
chr3 p24.1	1.101	1.396
chr3 p26.3	1.634	1.392
chr3 p24.2	1.038	1.344
chr3 q13.13	1.028	1.336
chr4 p15.31	0.928	1.321
chr3 q12.2	0.960	1.321

Supplemental Figure

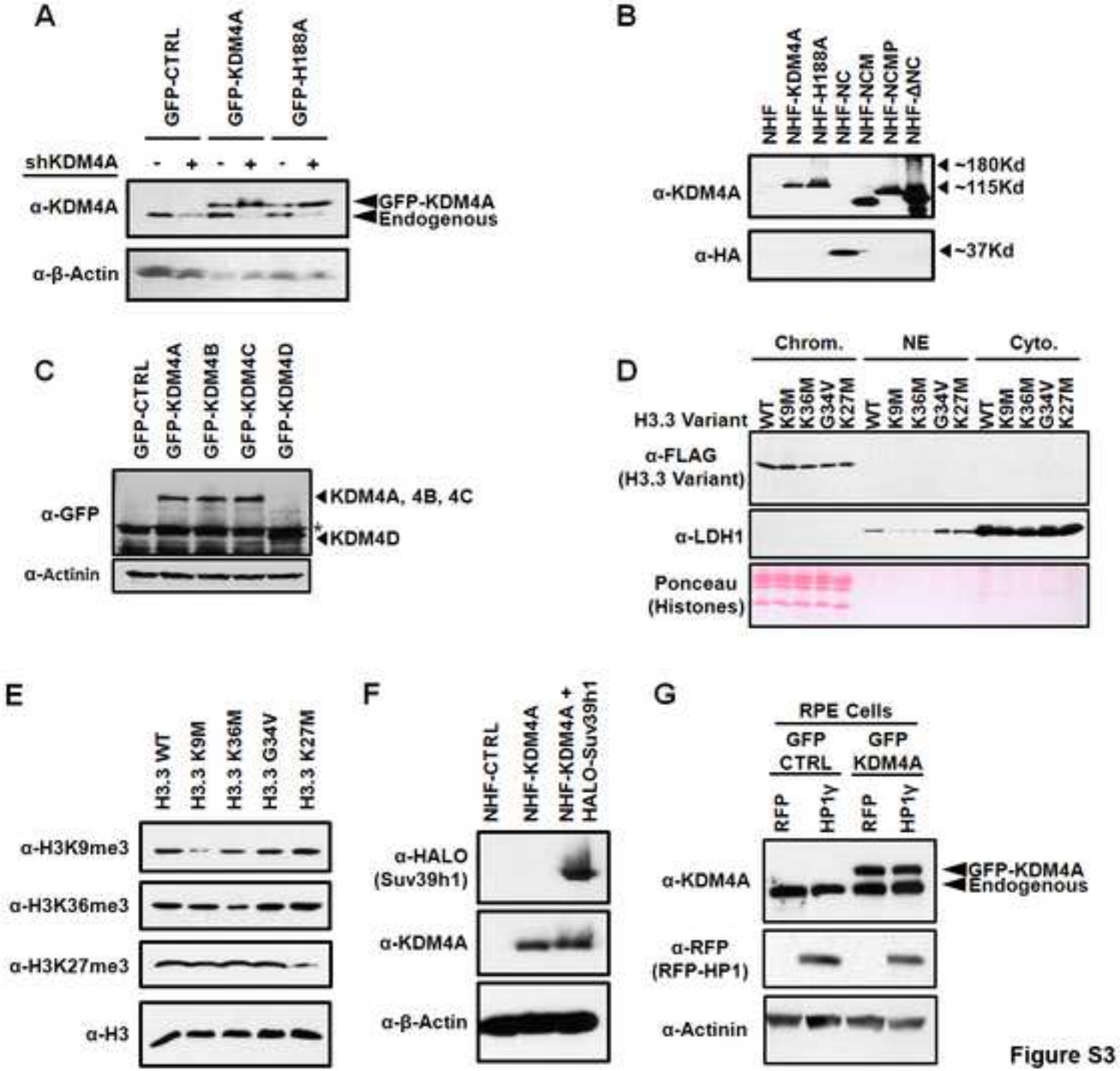

Figure S3

Supplemental Figure

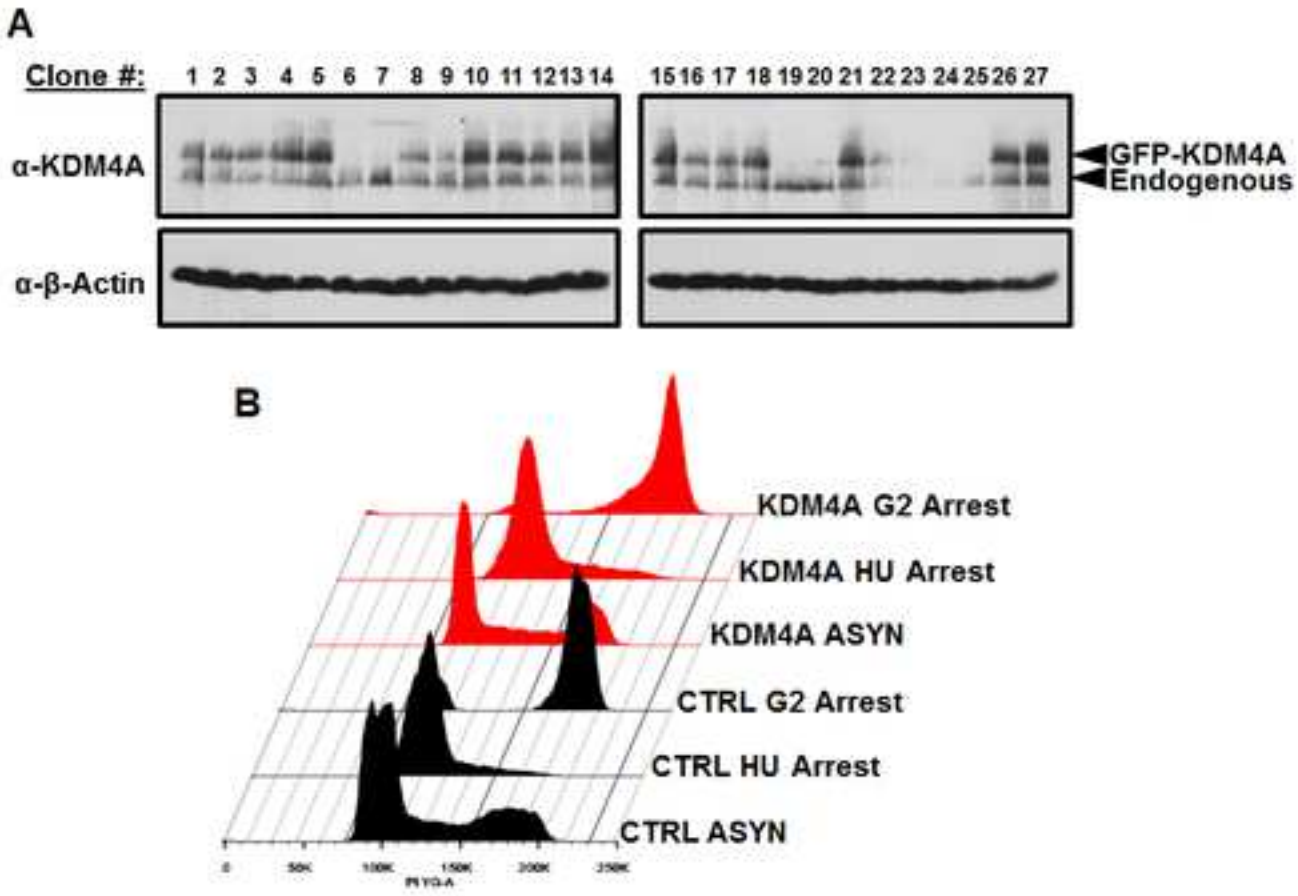

Figure S4

Supplemental Figure

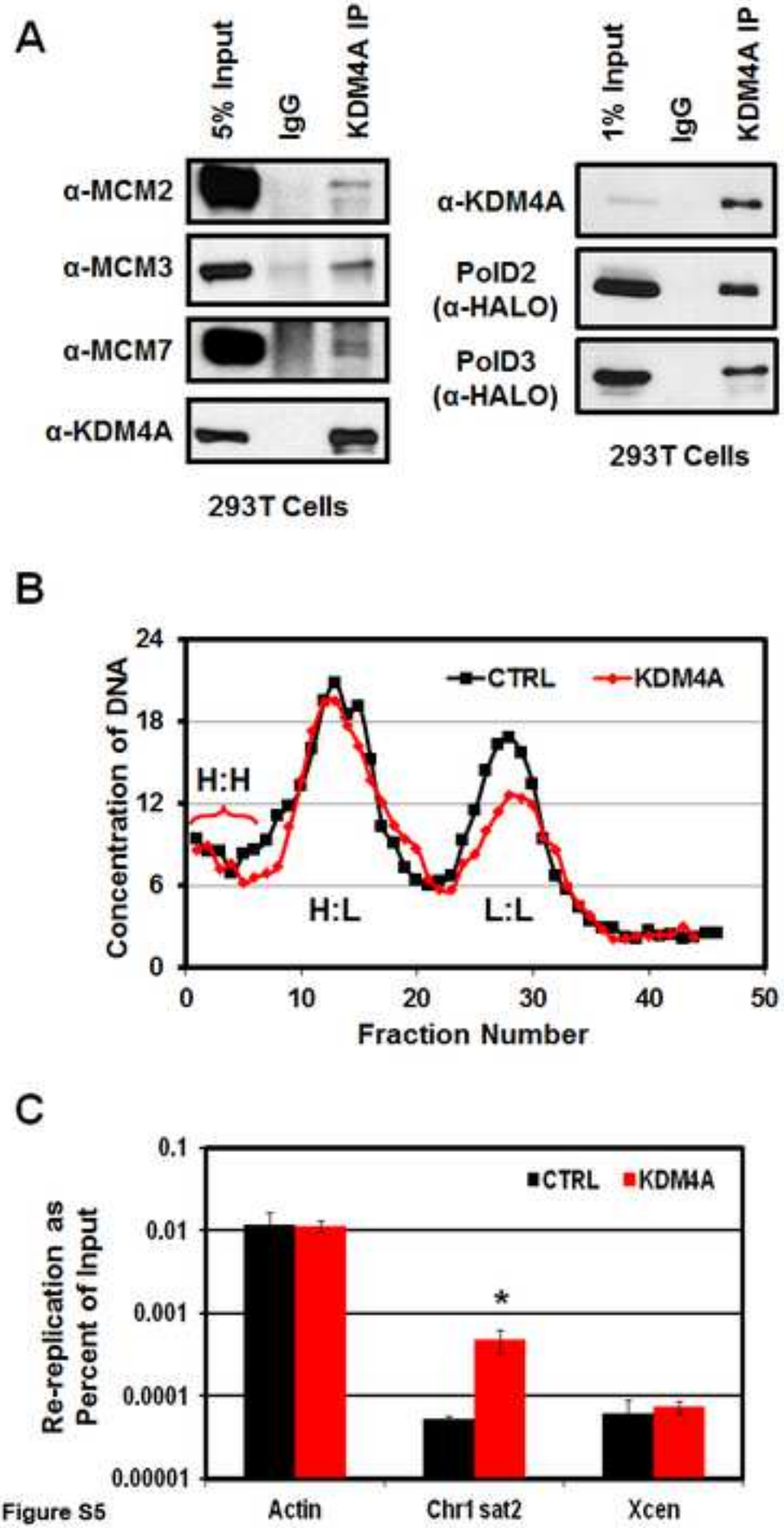

Figure S5

Supplemental Figure

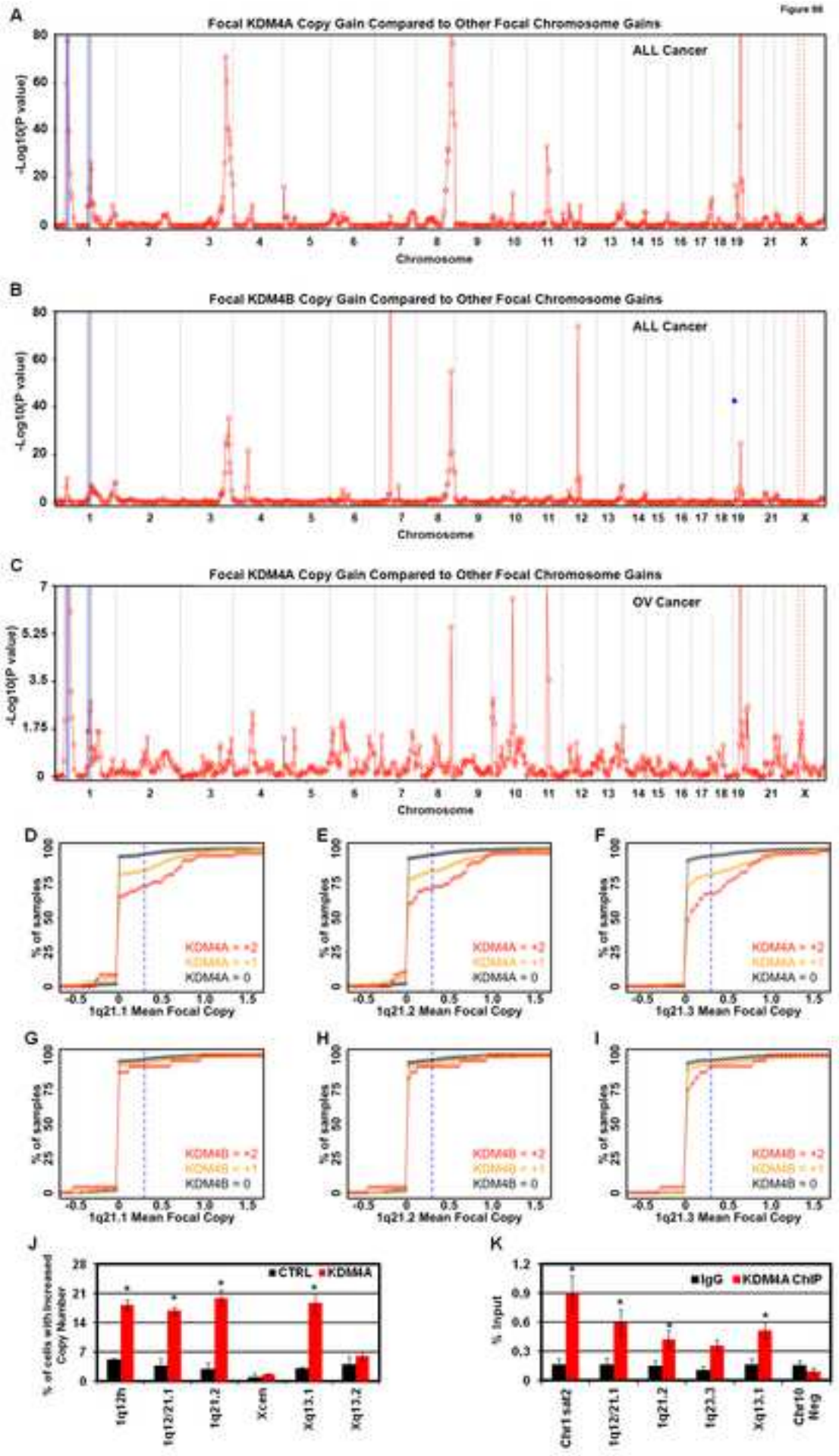

Supplemental Figure